

RIXS experiments under uniaxial strain

1 Strain-cell's principle

The recent development of strain-cells for in-situ strain measurements has allowed to discover new properties in electronic systems [1]. This new type of environment allows to compress or stretch a system along a single-direction, hence modifying, sometimes drastically, the electronic and magnetic properties of strongly correlated electron systems, e.g. in high- T_C and nematic superconductors [2, 3]. We are now intending to develop this new type of environment onto the RIXS spectrometer of ID20 with the aim of studying how the low-energy magnetic and d-d excitations in strong-spin orbit coupling systems evolves under uniaxial strain.

To that end, we choose to use a commercial CS200T uniaxial strain-cell from Razorbill instruments which consists in two piezoelectrics that can be drive through the application of an electrical voltage [4]. This commercial strain-cell allows to apply precise, and continuously tunable compressive and tensile strain in-situ at cryogenic temperature down to 50 mK. Moreover, the CS200T model allows to measure signal in transmission thanks to a transmission hole in the device allowing top and bottom 90° cone (see 1). In order to probe directly the displacement of the stacks, i.e. the strain applied onto the sample, parallel plate capacitive sensors are integrated with the purpose that a measurement of the capacitance between the stacks can be easily converted in displacement, hence in strain (the maximum being approximately 0.2 % depending on the sample). The capacitance is typically in the range of the pico-Farad.

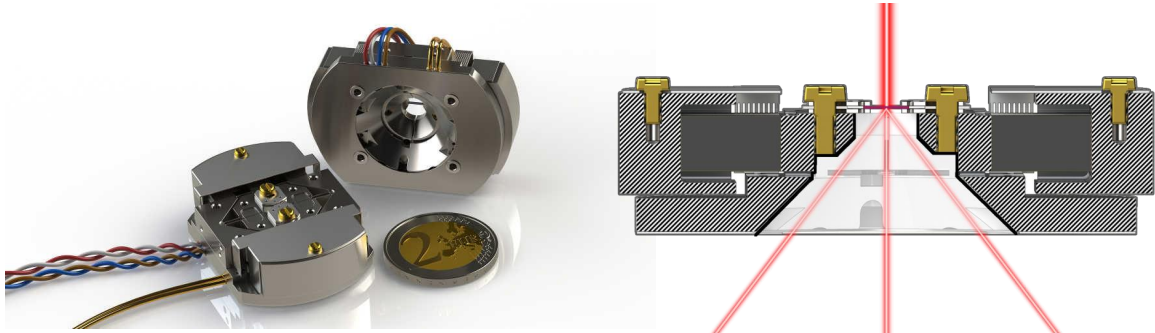


Figure 1: **CS200T strain-cell's principle:** Left: Picture of the Razorbill CS200T strain-cell, consisting in two titanate piezoelectric that can be drive through an apply voltage up to 200 V on both tensile and compressive stacks. Right: Transmission hole with top and bottom 90° apertures, allowing measurements in both reflection and transmission mode. Figures taken from Ref. [4]

2 Insertion of the strain-cell in a nitrogen cryostat for RIXS experiments on the ID20 beamline

To perform RIXS measurements under strain, the CS200T has been inserted into a nitrogen closed cryostat allowing to go down to 80 K. To that end, a copper based cold-finger has been designed so that the strain-cell could thermalize with the cryostat (see Fig. 2). The thermalization works remarkably well with a difference in temperature between the sample (probed with a Pt-sensor) and the exchanger of about 1 K. In order to drive the piezoelectrics, electronic connections have been made and plugged onto the four-quadrant (sink source) power supply of Razorbill, allowing to apply 200 V on each piezoelectric stacks. The capacitance reading was performed thanks to a LCR meter at 100 kHz and coaxial cables, allowing a precise measurement of the capacitance with a stability of ± 5 femto-Farad (see Fig. 2).

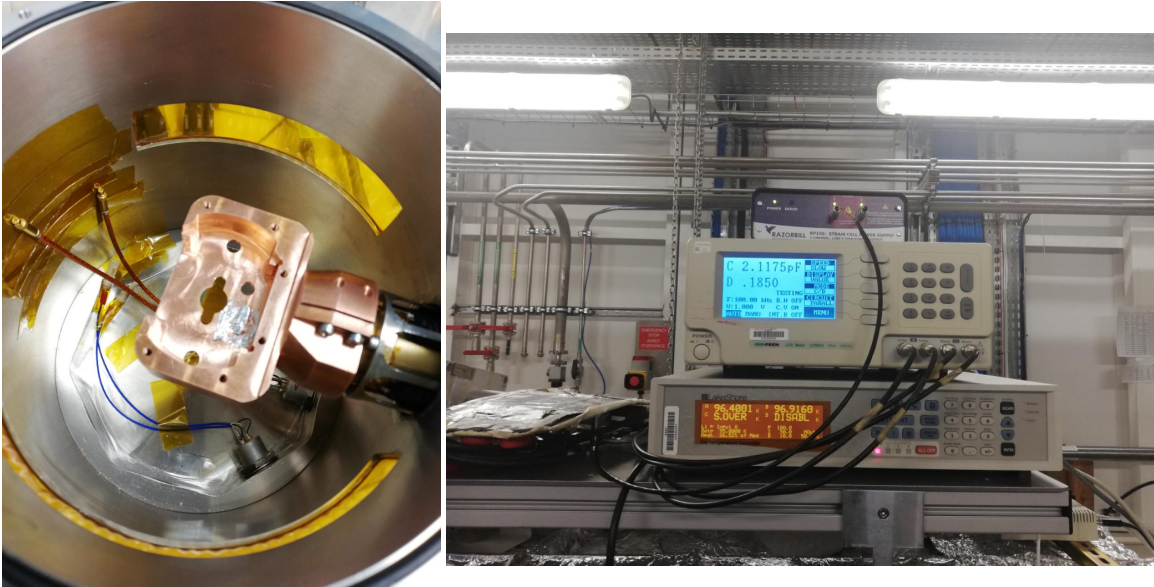


Figure 2: **Insertion of the strain-cell into a N_2 cryostat:** Left: Copper cold-finger designed for the CS200T strain-cell, allowing a good thermalization with the cryostat. Right: Razorbill power supply (top device) and LCR meter (middle device) plugged up to the strain cell inside the cryostat. The power supply allow to apply electrical voltage driving the piezoelectric stacks while the LCR meter allows a precise measurement of the displacement between the stacks. The lakeshore (down device) allows to measure the temperature of both exchanger and the strain-cell (measured with a Pt-sensor glued on it). Here the difference in temperature is around 0.3 K at 96 K, hence showing the very accurate thermalization of the strain-cell with respect to the exchanger.

3 Sample preparation of $Sr_3Ir_2O_7$ for RIXS measurements under strain

Measurements under strain require a certain shape for the sample. Indeed, they need to be bar shaped or ideally bottle necked shaped with typical dimensions of Length \times Width \times Thickness = 1 mm \times 0.1 mm \times 0.050 mm. We choose to perform a RIXS experiment under strain with the bilayer perovskite iridate $Sr_3Ir_2O_7$ that crystallizes in the tetragonal $I4/mmm$ space-group with lattice parameters $a = 5.52$, $b = 5.52$ and $c = 20.88$ (cite ..). This compound consists in bilayers of Ir^{4+} corned shared octahedra connected via bridging oxygens along the c -axis (see Fig. 3). This lead to the following magnetic ordering: the magnetic moments are antiferromagnetically (AFM) coupled within the ab plane (intralayer coupling), and AFM coupled along the c -axis between two layers (see Fig. 3). Samples were cut along the $[110]$ direction and glued onto the strain-cell with black stycast epoxy along the $[110]$ direction (see Fig. 3).

4 RIXS measurements on $Sr_3Ir_2O_7$ under strain; preliminary results

$Sr_3Ir_2O_7$ has been already extensively investigated by means of RIXS experiments (cite Marco) and its large spin-gap (100 meV) is ideal to start with such an experiment under strain. Besides, two magnons features (B and D features along $\mathbf{Q}=(H,H,28.5)$ in 4) have been found in this compound, the mechanism of their origin, in other words the low-energy Hamiltonian of this system, is still under debate [5, 6]. Indeed two models very different models were developed to explain the low-energy spin-dynamics of this system: on one hand, Kim et al. [5] who considered a spin-wave approach with dominant intralayer over interlayer interactions ($J \gg J_C$) and on the other hand, Moretti et al. [6] developed another approach by introducing a dimer-pseudospin interaction with $J_C \gg J$. Remarkably both approaches explain well the results observed so far.

To tackle this issue and to unveil the "true" low energy Hamiltonian of this system, we have performed very recently (February 2021) RIXS measurements on $Sr_3Ir_2O_7$ under strain by measuring RIXS spectra at the Iridium- L_3 edge ($E = 11.215$ keV) with an energy resolution $\Delta E = 25$ meV. The aim of this experiment was to either compress or stretch a $Sr_3Ir_2O_7$ sample, hence continuously tuning both intralayer

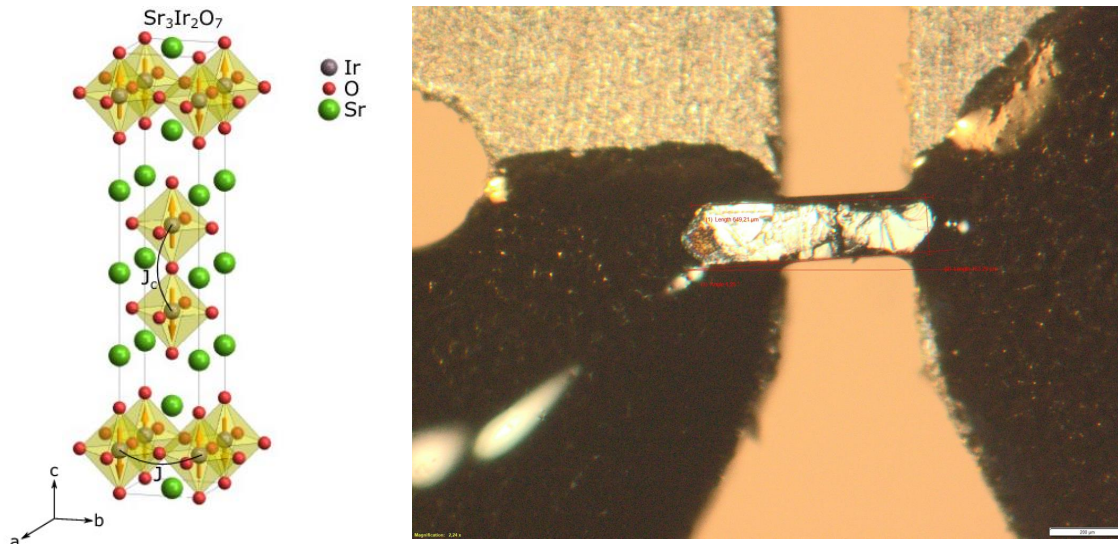


Figure 3: **$\text{Sr}_3\text{Ir}_2\text{O}_7$ sample preparation:** Left: Crystallographic and magnetic structures of $\text{Sr}_3\text{Ir}_2\text{O}_7$. The magnetic moments point towards the c -axis and are AFM coupled within the ab -plane (intralayer coupling J) and between two different planes (interlayer coupling J_C). Right: Picture of a bar shaped sample of $\text{Sr}_3\text{Ir}_2\text{O}_7$ with dimensions of Length \times Width \times Thickness \approx 0.650 mm \times 0.150 mm \times 0.100 mm. The strain is applied along the $[110]$ direction. The sample is glued onto the strain-cell with black stycast 2850FT epoxy.

J and interlayer J_C couplings. Assuming those change could be seen through dispersions, we have probed the strain-dependence of spectra around $\mathbf{Q}=(0,0,28.5)$ where the B and D magnons features are well separated (see Fig. 4 (a)). In order to confirm that strain was effectively applied onto the sample, the crystallographic Bragg peak $(0, 0, 32)$ was previously measured for different applied voltage (see Fig. 4 (b)). At +50 V (i.e. compressing the sample) the measured apply strain along the c -axis corresponds to $\epsilon_{cc} \approx 0.03\%$ which seems reasonable considering that the applied strain was along $[110]$, that the Poisson ratio might be around $1/3$ and that the epoxy might absorb a non-negligible part of the applied strain. Fig. 4 (c-d) show the RIXS spectrum obtained at $T = 100$ K and $\mathbf{Q} = (0, 0, 28.5)$ for $V = 0$ and $V = 50$ V (i.e. $\epsilon_{cc} \approx 0.03\%$). Magnetic excitations B and D are found around $E \approx 100$ meV (see Fig. 4 (d)). A shift in energy of around ≈ 15 meV of the magnonic excitations can be clearly seen on Fig. 4 (d) therefore demonstrating that the strain-cell is indeed modifying the magnetic interactions in this system.

References

- [1] Clifford W. Hicks et al. “Strong Increase of T_c of Sr_2RuO_4 Under Both Tensile and Compressive Strain”. In: *Science* 344.6181 (2014), pp. 283–285. ISSN: 0036-8075. DOI: 10.1126/science.1248292. eprint: <https://science.sciencemag.org/content/344/6181/283.full.pdf>. URL: <https://science.sciencemag.org/content/344/6181/283>.
- [2] H.-H. Kim et al. “Uniaxial pressure control of competing orders in a high-temperature superconductor”. In: *Science* 362.6418 (2018), pp. 1040–1044. ISSN: 0036-8075. DOI: 10.1126/science.aat4708. eprint: <https://science.sciencemag.org/content/362/6418/1040.full.pdf>. URL: <https://science.sciencemag.org/content/362/6418/1040>.
- [3] T. Kissikov et al. “Uniaxial strain control of spin-polarization in multicomponent nematic order of BaFe_2As_2 ”. In: *Nature Communications* 9.1 (Mar. 2018), p. 1058. ISSN: 2041-1723. DOI: 10.1038/s41467-018-03377-8. URL: <https://doi.org/10.1038/s41467-018-03377-8>.
- [4] URL: <https://razorbillinstruments.com/>.
- [5] Jungho Kim et al. “Large Spin-Wave Energy Gap in the Bilayer Iridate $\text{Sr}_3\text{Ir}_2\text{O}_7$: Evidence for Enhanced Dipolar Interactions Near the Mott Metal-Insulator Transition”. In: *Phys. Rev. Lett.* 109 (15 Oct. 2012), p. 157402. DOI: 10.1103/PhysRevLett.109.157402. URL: <https://link.aps.org/doi/10.1103/PhysRevLett.109.157402>.

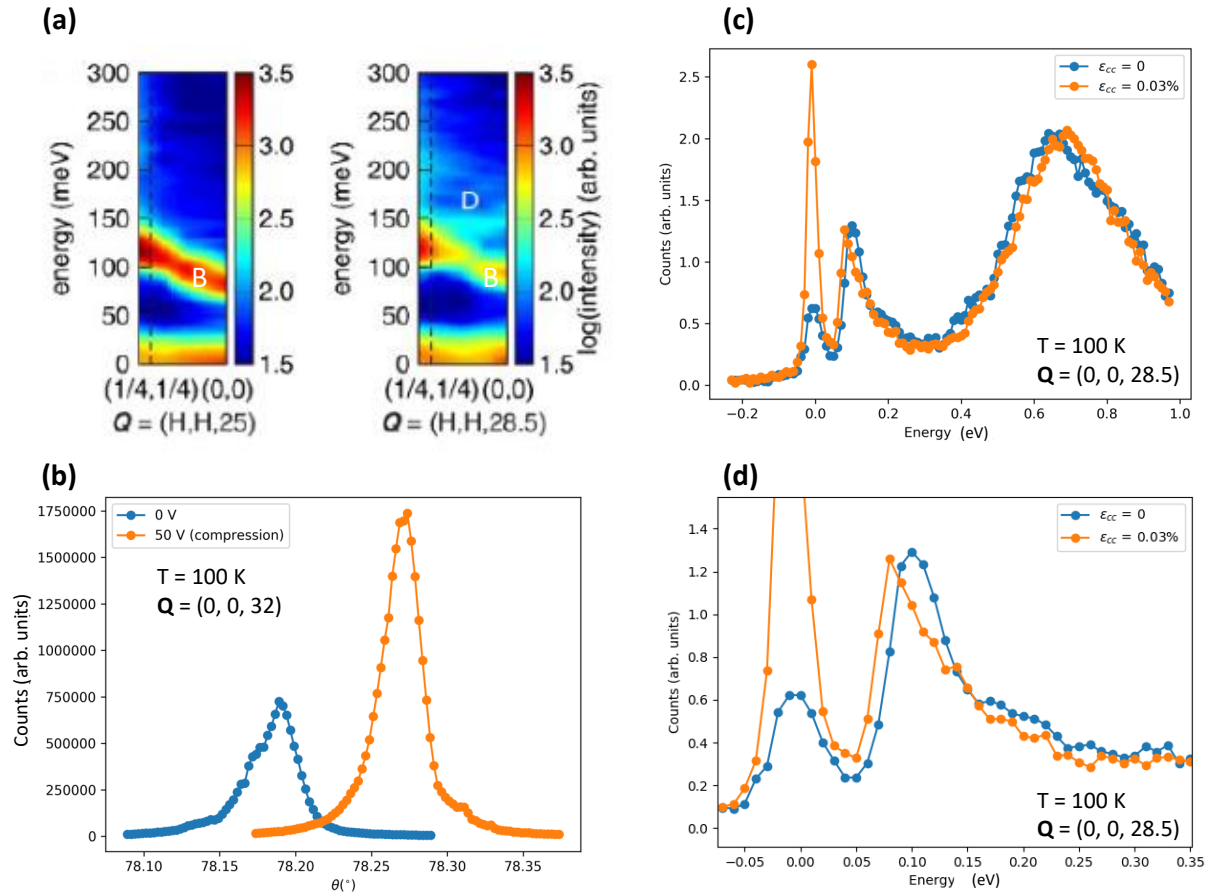


Figure 4: **RIXS measurements of $\text{Sr}_3\text{Ir}_2\text{O}_7$ under strain:** (a): Spin-dynamics of unstrained $\text{Sr}_3\text{Ir}_2\text{O}_7$ along $\mathbf{Q} = (H, H, 25)$ and $\mathbf{Q} = (H, H, 28.5)$. Two magnonic features B and D are visible for $L = 28.5$. Figure taken from Ref. [6]. (b): Crystallographic Bragg peak $(0, 0, 32)$ measured at $T = 100$ K at 0 V and +50 V (compression). The positive shift in θ corresponds to an apply strain along the c -axis of $\epsilon_{cc} = 0.03\%$. (c) Corresponding RIXS spectrum measured at 0 V and 50 V (unstrained and 0.03% strain along c respectively). (d) zoom of (c) around the magnonic excitations.

- [6] M. Moretti Sala et al. "Evidence of quantum dimer excitations in $\text{Sr}_3\text{Ir}_2\text{O}_7$ ". In: *Phys. Rev. B* 92 (2 July 2015), p. 024405. DOI: 10.1103/PhysRevB.92.024405. URL: <https://link.aps.org/doi/10.1103/PhysRevB.92.024405>.